Precise control of dissolved oxygen in bioreactors – a model-based geometric algorithm

James Gomes[a,*], Anil S. Menawat[b]

[a]*Department of Biochemical Engineering and Biotechnology, Indian Institute of Technology, Delhi, Hauz Khas, New Delhi 110 016, India*
[b]*Advanced Solutions and Know-How 1426, Hidden Creek North Saline, MI 48176, USA*

Received 6 March 1998; accepted 21 December 1998

Abstract

In this paper, we develop a Model-Based Geometric Control Algorithm (MGA) for controlling the dissolved oxygen concentration in fermentation processes. The algorithm is developed on a generic system description which encompasses a wide range of models commonly used to describe bioprocesses. Consequently, the algorithm we have derived will apply to any process whose model fits the generic description. The algorithm uses information contained in the shape (geometry) of the profile of the state variables as they evolve in time to adapt to process variations. There are two components in the algorithm, an estimator and a controller, whose functions complement each other. The estimator component of the algorithm predicts the states and the parameters of the system one time step ahead. Since the estimator is *deadbeat*, the algorithm converges in a finite number of steps. The control component of the algorithm uses the states predicted by the estimator and executes a control action so that predicted error falls below a desired level. Simulations for comparing the performance of the IMC, PI and MGA controllers are presented. The MGA was implemented on-line to control the dissolved oxygen in an aminoglycoside antibiotic production process by a *Streptomyces* and the results of its performance are also presented.

Keywords: Nonlinear control; Dissolved oxygen; On-line; Streptomyces; Set-point tracking; Spectinomycin

1. Introduction

Designing an effective control strategy for controlling dissolved oxygen in a bioprocess requires careful analysis. Oxygen requirements for a particular product depends on the energetics of the pathway leading to the product. Hence, aeration which is a primary energy input to the process, is an important design parameter. Since most antibiotic fermentations involve mycelial species, the resulting broths are highly viscous. This high viscosity of fermentation broths leads to the development of stagnant zones and dissolved oxygen gradients in the vessel. Consequently, the microorganisms in large industrial fermenters (200,000 l) experience fluctuating dissolved oxygen concentrations in their micro-environments. Therefore, controlling the aeration rate efficiently can contribute to increasing the overall productivity of the process.

Several studies concerning the effect of dissolved oxygen on the productivity of antibiotic (Chen & Wilde, 1991; Rollins, Jensea & Westlake, 1988, 1989; Rollias, Jensen, Wolfe & Westlake, 1990; Yegneswaran, Gray & Westlake, 1988; Yegneswaran, Gray & Thompson, 1991a, 1991b) demonstrate that oxygen participates in the regulation of the key biosynthetic enzymes and thus the final yield of the antibiotic. Rollins et al. (1990) observed that by maintaining the dissolved oxygen concentration at either 50 or 100% throughout the fermentation increased the final titers of Cephamycin C two-fold and three-fold, respectively, in comparison to fermentations without dissolved oxygen control. In the fermentation of Cephamycin C and Cephalosporin C antibiotics, reduction in the oxygen supply leads to an accumulation of the intermediate Penicillin N. This suggests that a higher oxygen concentration in the liquid phase increases the synthesis of enzymes catalyzing the conversion of Penicillin N to Cephamycin C. Riege, Blasig, Muller, Heidenreich and Bauch (1989) demonstrated that reduced oxygen decreased protein formation and carbon incorporation in *Candida maltosa* using *n*-alkanes as

Notation

A constant matrix approximation of $A(t)$ over one sampling period
$A(t)$ approxmation of the matrix of Lie derivatives with respect to f
B constant matrix approximation of $B(t)$ over one sampling period
$B(t)$ approxmation of the matrix of Lie derivatives with respect to g
$f(x)$ n-dimensional vector of the process kinetics
$g(x)$ n-dimensional vector of the process transport
$h(x)$ observation function
i subscript of matrix elements having values 1, 2, ..., α
k value of sampling period
$L_f h$ Lie derivative of h in the direction of f
$L_g h$ Lie derivative of h in the direction of g
n dimension of the state vector
Δt sampling time interval
t_k time at any sampling instant k
u process input
x n-dimensional vector of states
y process output

Greek letters

α relative order of the system
Γ convolution term
δ sampling time interval
ζ prejection for evaluating the derivative
ϕ combined matrix of states and input
Φ exponential term
θ vector of all parameters

carbon source. Whereas, low levels of dissolved oxygen concentration enhanced the productivity of Pullulan by *Aureobasidium pullulan* (Wecker & Onken, 1991) and ethanol by *Pichia stipis* (Grootjen, van der Lans & Luyben, 1990; Preez, du van Driessel & Prior 1989). On the other hand, the production of β-1,3-glucan by *Alcaligenes faecalis* (Lawford & Rousseau, 1989) and the production of clavulanic acid by *Streptomyces clavuligerus* (Scott, Sladen, Maidment, Rashid, Pratsis & Perry, 1980) require high oxygen transfer rates.

Interacting effects between oxygen and other process variables occur at the fundamental level of energy transduction. Siano and Mutharasan (1991) studied the NADH fluorescence and oxygen uptake responses of mammalian cells to metabolic events induced by the inhibition of respiration and pulsing of glucose and glutamine. They examined the inhibition with a 0–5 μM rotenone step change during batch cultivation. Step changes in the dissolved oxygen between 25 and 0% air saturation induced aerobic–anaerobic–aerobic transitions. The oxygen uptakes rates changed significantly during the pulse and step experiments, suggesting corresponding changes in the cellular metabolism. Therefore, it is not surprising that the oxygen dynamics reflect the changes in the environmental conditions because oxygen uptake is intricately linked to cellular metabolism. Further, dissolved oxygen concentrations change about 10 times faster than the cell mass and substrate concentrations. Thus, oxygen is the most important physiological variable for control and optimization of fermentations.

In the early 1980s bioprocess control strategies depended on the law of conservation (Cooney, Wang & Wang, 1977; Mou & Cooney, 1983) or on filtering techniques (Stephanopoulos & San, 1984; Wang & Stephanopoulos, 1984) to obtain indirect measurements of state variables. Sensor technology had not developed sufficiently to fulfill the needs of the control engineer. Hence, these techniques were applied successfully in many bioprocesses where it was not possible to measure the desired variable. Cooney et al. (1977) used elemental balances to estimate unmeasured states from measured ones. Based on this philosophy, they implemented control strategies to maintain the maximum yield on substrate and the highest volumetric productivity (Swartz & Cooney, 1979; Wang, Cooney & Wang, 1979).

Later, researchers focussed on the development of model-based adaptive controllers using the Kalman filter and the extended Kalman filter. These filters helped to identify the model parameters and the unmeasured states (Shimizu, Takamatsu, Shioya & Suga, 1989; Stephanopoulos & San, 1984). There are a few difficulties with this approach. The Kalman filter requires a priori information for on-line implementation. The availability of the information required cannot always be ensured. This is particularly a serious problem with models used for bioprocesses because parameters are difficult to identify (Holmberg & Ranta, 1982; Holmberg, 1982). Also, it is sometimes difficult to guarantee that the desired state estimates are observable with the process measurements used in the filter.

These problems led to further developments in model-based control for bioprocesses. Bastin and Gevers (1980) developed an adaptive observable canonical form (AOCF) observer for nonlinear systems transformable into the observable form. Other researchers combined adaptive estimation with control for bioprocesses (Chattaway & Stephanopoulos, 1989; Johnson, 1985; Massimo, Saunders, Morris & Montague, 1989; Munack & Posten, 1989; Pomerleau & Perrier, 1990; Pomerleau, Perrier & Dochain, 1989). However, some extent of these problems persist in these methods. Recent developments in hybrid control systems (Lübbert & Simutis, 1994; Zhang, Reid, Litchfield, Ren & Chang, 1994; Ge & Lee, 1997)

which combine artificial neural networks with expert systems, fuzzy controllers or adaptive schemes, answer some of these problems. In a different approach, some researchers (Gomes & Menawat, 1992; Proll & Karim, 1994) applied nonlinear systems theory for developing estimation and control strategies for bioprocesses. We will follow the second route and apply nonlinear systems theory to develop an algorithm for controlling dissolved oxygen in bioreactors.

The Model-Based Geometric Algorithm (MGA) we have developed using nonlinear systems theory, incorporates two components — a predictor and a controller. The predictive component estimates the dissolved oxygen one time step ahead based on the *geometry* of the process (profile of state variables in time). The control component uses this estimate to compute a control action that should be implemented to minimize the error predicted for the next time interval. In some sense it may be classified as hybrid between an adaptive controller and a self-tuning controller. In this paper, we shall first present the development of the algorithm. We shall prove theoretically that the algorithm will converge in a finite number of time steps and also show its convergence characteristics through simulations. Next, we shall compare the performance of the algorithm with the performance of the IMC and PI controllers through several simulation experiments. Finally, we shall present the results of its performance when implemented on-line for controlling the dissolved oxygen in spectinomycin production.

2. Development of the algorithm

Below we develop the MGA for a single-input–single-output (SISO) case. The multiple-input–multiple-output case readily follows but is not discussed here. The MGA is designed for a general system description that does not depend on the details of process kinetics and transport. In this sense, the algorithm is model based. The only requirement we impose is that the input (control) variable should be able to manipulate the output (measurement). In other words, the process must exhibit controllability. This may be justified by physical arguments instead of mathematical analysis. In this paper our interest is in developing a control algorithm for dissolved oxygen control. For this case, the output would be the measurement obtained from the dissolved oxygen probe, and the input would be the air flow rate. However, we keep the derivation general and do not explicitly define what and how many states the system has. The designer may specify his own model so long as it satisfies the general model description given below.

$$\dot{x} = f(x) + g(x)u,$$
$$y = h(x). \tag{1}$$

Here x is an n-dimensional vector of the states of the process. The symbols y and u represent the output and the input variables. Eq. (1) is the law of conservation with $f(x)$ describing the kinetic phenomenon (the natural drift). The input is the net flux into the system with its quality defined by $g(x)$. The output is the means to observe the behaviour which may be one of the states of the system or some measure of it. The specific choice of the functions f, g and h are not relevant for the derivation. However, they must be sufficiently smooth and differentiable. This is not restrictive by any means because most of the physical system descriptions fall into this category.

Eq. (1) is an appropriate form to develop the MGA for fermentation applications since most fermentation models can be reduced to this form. Table 1 contains a few of the published fermentation models. The table shows only the kinetic terms. Addition of the transport terms complete the model for the fermenter. The transport term describes the physical inputs and outputs like air sparging, nutrient addition, and chemostat outlet. Kinetic models in Table 1 are variations of the Monod equation. Such descriptions satisfy the criterion of sufficient smoothness and differentiability.

To find the relation between the input and the output we begin by differentiating the output y with respect to time. We continue the process of differentiation until the input u appears explicitly in the relation. The number of differentiations required is called the *relative order* α of the system. Thus, differentiating the output y successively α times we obtain

$$y = h(x),$$
$$\dot{y} = L_f h(x),$$
$$\ddot{y} = L_f^2 h(x),$$
$$y^{(\alpha-1)} = L_f^{\alpha-1} h(x),$$
$$\vdots$$
$$\vdots$$
$$y^{(\alpha)} = L_f^{\alpha} h(x) + L_g L_f^{\alpha-1} h(x) u, \tag{2}$$

where the symbols L_f and L_g which denote the Lie derivatives of the measurement $h(x)$ with respect to the vector fields f and g are defined by

$$L_f h = \langle \mathrm{d}h, f \rangle,$$
$$L_f^{\alpha} h = L_f (L_f^{\alpha-1} h) = \langle \mathrm{d}L_f^{\alpha-1}, f \rangle, \tag{3}$$

and

$$\langle \mathrm{d}h, f \rangle = \frac{\partial h}{\partial x_1} f_1 + \cdots + \frac{\partial h}{\partial x_n} f_n.$$

Since the transformation [Eq. (2)] which relates the outputs to the inputs of the system is geometric, there is no loss of information and the essential characteristics of the

Table 1
Kinetic structures of fermentation models

Monod (1942)	$\mu(S) = \frac{\mu_m S}{K_m + S}$
Tessier (1942)	$\mu(S) = \mu_m\left(1 - \exp\left(-\frac{S}{K_m}\right)\right)$
Moser (1958)	$\mu(S) = \frac{\mu_m S^\lambda}{K_m + S^\lambda}, \lambda > 0$
Contois (1959)	$\mu(S, C) = \frac{\mu_m S}{K_c C + S}$
Powell (1967)	$\mu(S) = \frac{\mu_m}{2K_m}(K_m + S - \sqrt{K_m + S^2 - 4K_m S})$
Peringer, Blachere, Corrieu and Lane (1972)	$\mu(S, A) = \mu_m^a \frac{S}{K_m + S}\left(\frac{A}{K_a + A} + \frac{1}{1 + K_b A}\right) + \mu_m^b$ with $2\mu_m^a + \mu_m^b = \mu_m$
Jackson and Edwards (1975)	$\mu(S, H^+) = \frac{\mu_m S}{\left(1 + \frac{K_2}{H^+} + \frac{H^+}{K_1}\right)(K_m + S + S^2/K_i(1 + K_3/H^+))}$
Olsson (1976)	$\mu(S, A) = \mu_m \frac{SA}{(K_m + S)(K_a + A)}$
Dourado and Calvet (1983)	$\mu(S, P) = \mu_m \frac{S}{(K_m + S + S^2/K_i)} \frac{K_p}{(K_p + P)}\left(1 - \frac{P}{P_l}\right)$
Williams, Yousefpour and Swanick (1984)	$\mu(S, A, P) = \left(\frac{K_1 S}{K_m + S} + \frac{K_2 P}{K_p + P}\right)\left(\frac{A}{K_a + A} + K_3 A - K_4\right)$

S = substrate concentration, C = cell mass concentration, P = product concentration, A = dissolved oxygen concentration, H^+ = hydrogen ion concentration, $K_{(\text{anysubscript})}$ = constant, μ = specific growth rate, μ_m = maximum specific growth rate.

system remain imbedded in the transformation. To implement this algorithm on-line we need to consider the behaviour of Eq. (2) over a reasonable sampling interval $\Delta t = \{t | t_k \leqslant t \leqslant t_{k+1}, k = 0, 1, 2, \ldots\}$. For real systems, it is always possible to define this Δt neighbourhood in such a way that the conditions of geometric reciprocity transformation are not violated. This is because real systems are distinguishable systems. Further, they are bounded and approximate to linear behaviour in small neighbourhoods. For example, an aerobic fed-batch fermentation may have an initial cell mass concentration of 0.5 g/l glucose concentration of 5 g/l with an input of constant glucose feed rate of 0.01 g/min. Normally, in bioprocesses all state variables have defined initial and final conditions, and inputs that are bounded. Hence, without loss of generality, we can replace the Lie derivative terms of Eq. (2) with their estimates in the sampling interval Δt in the form

$$\dot{y}^{(\alpha-1)} = A(h(x(t)) + B(h(x(t), u(t)). \tag{4}$$

Noting that the parameter B incorporates u the control variable, the derivation of the geometric control algorithm proceeds through a number of simple algebraic steps. Dropping the successive differentiation notation $(\alpha - 1)$, we simplify Eq. (4) for the periodic sampling interval Δt, $t_k = k\Delta t$ as

$$y(k\Delta\, t + \Delta t) = \Phi(\Delta t) y(k\Delta t) + \Gamma(\Delta t),$$

with

$$\Phi(\Delta t) = \mathrm{e}^{(A\Delta t)}, \tag{5}$$

and $\Gamma(\Delta t) = \int_0^{\Delta t} \mathrm{e}^{(A\Delta t)} B(\tau)\, \mathrm{d}\tau$.

In reasonably small intervals of time, such as the response time of the dissolved oxygen probe (compared to cell doubling time), we can assume that $A(h(x(t)))$ is adequately represented by the interaction of effect of the input $y(k\Delta t)$ and the nonlinear system contribution for the current time interval $\Phi(\Delta t)$. The nonlinear interaction of the input with the system is represented by the estimate for the current time interval by $\Gamma(\Delta t)$. Since the estimate A of $A(h(x(t)))$ remains constant during the sampling interval, the exponential term $\mathrm{e}^{(A\Delta t)}$ is easily evaluated with the Caley–Hamilton theorem. Evaluating the derivative accurately is a determining factor for the performance of the MGA controller. Similarly, the estimate B of $B(h(x(t)), u(t))$ remains constant during the interval. The subsequent steps of the derivation of the geometric algorithm are simplified by defining the convolution

$$\zeta_n = \int_0^{\Delta t} \mathrm{e}^{A\tau} \tau^n\, \mathrm{d}\tau. \tag{6}$$

This algebraic manipulation gives a far superior estimate of the derivative than the conventional Euler difference or central difference approximation. It also simplifies the evaluation of $\Gamma(\Delta t)$. Substituting ζ into Eq. (5) results in

$$y(k+1) = (I + A\zeta_0)y(k) + \sum_{i=0}^{\alpha} \zeta_i b_i. \tag{7}$$

The existence of A^{-1} is necessary for the convergence of the algorithm. If system (1) is observable with the chosen observation function $h(x)$, then Eq. (2) and hence Eq. (4) is invertible. Computation of ζ is feasible only if the matrix A^{-1} exists. Without loss of generality, we can rewrite Eq. (4) as

$$\dot{y} = \phi^{\mathrm{T}}\theta \tag{8}$$

and hence evaluate the parameters from

$$\theta = (\phi\ \phi^{\mathrm{T}})^{-1}\phi\dot{y}. \tag{9}$$

A singular value decomposition is employed for estimating the parameters A and B. The state and control variables and then computed from the nonlinear terms appearing in the input–output linearized system [Eq. (2)].

We initialize the algorithm by filling in the data window with the required measurements. A suitable sampling period ensures that the initial data reflects the process dynamics. For calculating the *initial* values of the derivatives $\dot{y}$, we use a simple Euler's approximation. *Subsequent* values of the derivatives $\dot{y}$ are computed from the projection ζ_0. Next, we estimate the parameters from which the states are predicted one time step ahead. Simultaneously, the algorithm calculates a new control action which minimizes the error between the control variable and the desired set point one time step ahead. The projection ζ_0 is then evaluated to calculate the derivatives $\dot{y}$ for the next cycle. The data window is updated by dropping the oldest value and including the current data point. Through the information contained in the data window the algorithm retains the past information of the system. Since this information is updated at every sampling, it enables the algorithm to adapt to changes in the process. The cycle repeats with the estimation of a new parameter set and control action. Fig. 1 illustrates the adaptive–predictive behaviour and the predicted error minimizing action of the algorithm.

The geometric control algorithm satisfies the general linear system [Eq. (8)]. The algebraic solution of the parameters of this system is Eq. (9). The mathematical solution of Eq. (9) is straightforward. The parameter estimates of equations with this structure converge in a finite number of steps and is commonly known as a *deadbeat estimator*. Since in our case, the continuous parameters $A(t)$ and $B(t)$ were replaced by their estimates A and B, the convergence of Eq. (9) depends on the existence of the estimates A and B. Since the system [Eq. (1)] is observable with $h(x)$ and controllable with u [Eq. (2)], it is also invertible (Hirschorn, 1979; Hermann & Krener, 1977; Jurdjevic, 1970). By superimposing the bounded property of the system (Rivlin, 1981), it can be shown that the estimates A and B exist for the sampling interval Δt. Hence, the algorithm must converge within a finite number of time steps. The control action is computed from the analytical solution of Eq. (9). However, the control action is one-sided and so the rate of decay depends on the dynamics of the process.

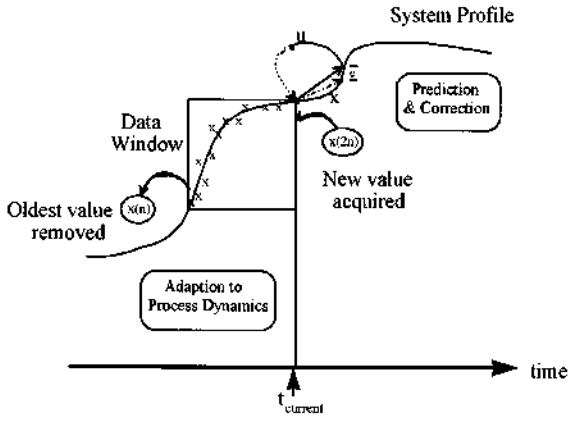

Fig. 1. The adaptive-predictive structure of the Model-Based Geometric Algorithm.

Estimation of the system parameters and control of the process are combined into one algorithm. The estimated parameters and control action are constant over the sampling interval. Since the control variable is imbedded in one of the parameters, namely B, new control values are obtained after evaluation of the parameters for any particular sampling interval. The convergence characteristics of the algorithm is examined with several simulation experiments. We used a general growth model to conduct the simulations. The simulation experiments employ the Bulirsch–Stoer integration routine, recommended for high accuracy solutions to ordinary differential equations with minimum computational effort (Stoer & Bulirsch, 1980).

We tested the convergence properties of the algorithm by implementing it on a dissolved oxygen control simulation experiment. Further, we assumed the presence of 5% multiplicative noise in the measurements. In this experiment the correct starting concentration for dissolved oxygen was 50% saturation. However, to test the algorithm, we assumed that the algorithm inadvertently acquired the wrong initial condition of 60% saturation. Under these circumstances, we required the algorithm to predict and control the dissolved oxygen concentration by manipulating the air flow rate. We observed, that the algorithm converged quickly to the true values (Fig. 2). The prediction of the algorithm and the manipulated variable, the air flow rate, computed using the predicted values of the dissolved oxygen concentration are also

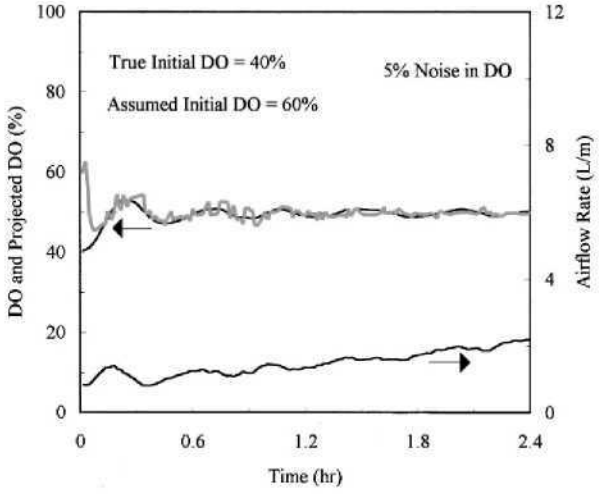

Fig. 2. Convergence characteristics of the MGA. Step down convergence from an incorrect initial value of 60% instead of 40% to set point of 50%.

Table 2
Comparison of the performance of the IMC, PI and MGA controllers

Control	Parameters		T_{CON}	σ
	Calculated	Tuned		
IMC	$K_c = 0.5445$ (l m^{-1} DO%$^{-1}$)	$K_c = 1.6033$ (l m^{-1} DO%$^{-1}$)	0.50 (h)	3.090
	$\tau_c = 0.0090$ (h)	$\tau_c = 0.0500$ (h)		
	$\tau_I = 0.0824$ (h)	$\tau_I = 0.0824$ (h)		
	$\tau_D = 1.36 \times 10^{-3}$ (h)	$\tau_D = 1.36 \times 10^{-3}$ (h)		
PI	$K_c = 2.263$ (l m^{-1} DO%$^{-1}$	$K_c = 25.00$ (l m^{-1} DO%$^{-1}$)		
	$\tau_I = 8.61 \times 10^{-3}$ (h)	$\tau_I = 9.0 \times 10^{-3}$ (h)	0.10 (h)	2.797
MGA	—	—	0.75 (h)	1.053

presented in the same figure for comparison. In fact, even with a default initial condition of 0% saturation, the algorithm converges quickly to the true values (see Fig. 11).

In the ideal situation where noise is absent, the predicted dissolved oxygen concentration converges to the true value in approximately 0.2 h. Whereas, with 5% noise added the predicted values converge within acceptable limits of the true value in about 0.3 h. Since the rate of decay of the dissolved oxygen concentration depends on the oxygen demand only and the fermentation is initially sensitive to air input, we observe oscillations during the initial period. In pH control where the rate of decay can be manipulated by adding acid, these initial oscillations are completely removed (see Figs. 10 and 11). Therefore, if nitrogen is used to control the overshoot of oxygen concentration in the liquid phase, the magnitude of observed oscillations would be minimized.

3. Comparison of the algorithm with IMC and PI control

We now compare the performance of the geometric algorithm to the classical PI control and the more recent internal model control (IMC) strategy (Morari & Zafiriou, 1989; Rivera, Morari & Skogestad, 1986). In the IMC methodology, the nature of the process model assumed determines the controller settings. Usually, a simplified model such as a first-order or second-order process with dead time is assumed and the controllers settings are obtained in terms of the model parameters which are obtained from simple experiments. Consequently, the IMC enjoys two distinct advantages over the PID design methodologies: (1) It explicitly accounts for model uncertainty, and (2) acquires robustness to process changes and plant-model mismatch. Here, for the IMC controller, we describe the dissolved oxygen dynamics using a first-order model with dead time. The PID controller settings for the IMC controller were determined and implemented to control the dissolved oxygen concentration. Similarly, we determined the controller settings for the classical PI controller based on the Cohen–Coon criteria (Cohen & Coon, 1953).

The process gain, the time constant and the dead time for the first-order dead time model were obtained from the transient response in the dissolved oxygen concentration for a step change in air flow rate. The initial controller setting were obtained from these parameters. These initial settings of the IMC and PI controllers were fine tuned to satisfactory performance (Table 2).

3.1. Set point control

Although simulations were conducted for several different set point value of dissolved oxygen ranging from 20 to 80%, only result for the 50% dissolved oxygen set point will be presented here for comparing the performance of the IMC, PI and MGA controllers. The simulation condition in each case was identical. The ideal situation without noise was used for fine tuning the IMC and PI controllers, starting from the initial settings. The MGA controller being adaptive did not require tuning. The IMC and PI controllers were considered suitably tuned when satisfactory step response characteristics were obtained for the ideal situation. The IMC, PI and MGA controllers were then implemented for control where a 5% multiplicative random noise was incorporated in the dissolved oxygen measurements. A time frame of 2.4 h is sufficient to compare the transient performance of the three different strategies.

Fig. 3 shows the performance of the IMC controller when 5% random multiplicative noise isu incorporated in the dissolved oxygen measurements. We notice rapid changes in the air flow rate. The IMC control action as observed in the air flow rate values do not appear to

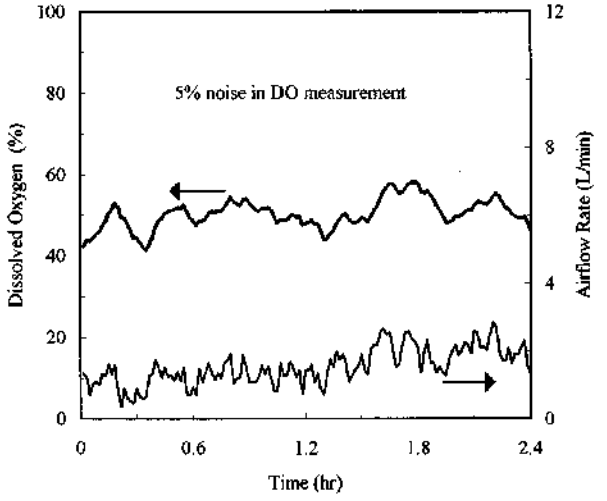

Fig. 3. Dissolved oxygen control at 50% with IMC controller. Dissolved oxygen and air flow rate profiles when there is 5% noise in the measurements.

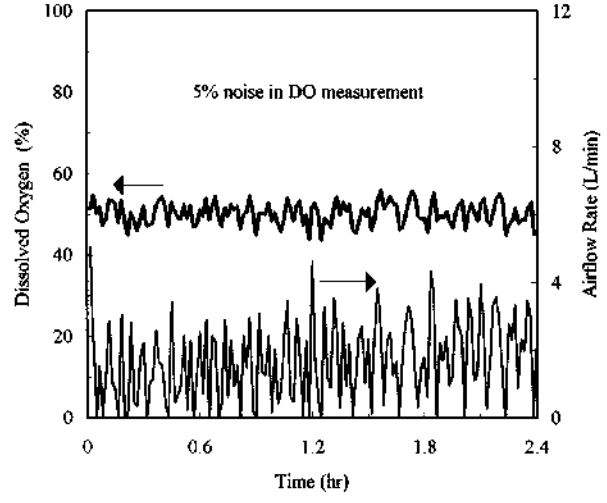

Fig. 4. Dissolved oxygen control at 50% with PI controller. Dissolved oxygen and air flow rate profiles when there is 5% noise in the measurements.

converge to a specific "solution" profile. Similarly, the classical PI controller shows very rapid changes in the air flow rate (Fig. 4). Such rapid changes in the control action normally indicate potential danger of loosing control over the process. A comparison of Figs. 3 and 4 show that the PI control action is more erratic than the IMC controller.

Unlike the IMC and PI controllers the MGA converges distinctly to a solution profile of the air flow rate (Fig. 5). A comparison of Figs. 3–5 reveals that the MGA control action is smoother than the IMC or classical PI controllers. We attribute this to the following features of the algorithm:

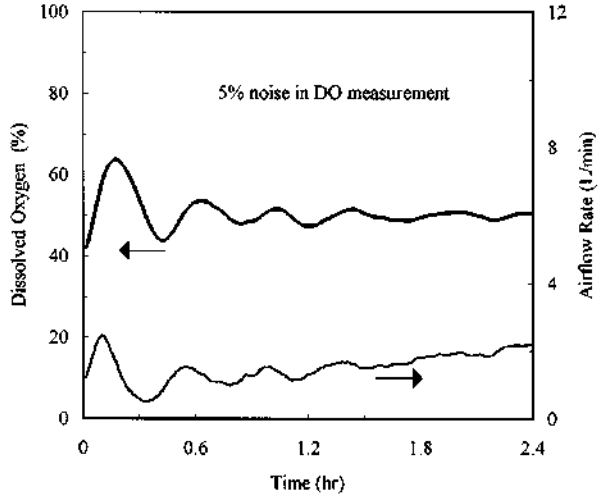

Fig. 5. Dissolved oxygen control at 50% with MGA controller. Dissolved oxygen and air flow rate profiles when there is 5% noise in the measurements.

(i) The algorithm is adaptive. The parameters estimated in A and B change rapidly with the process dynamics.
(ii) The algorithm is predictive. It predicts the controlled variable using a special projection ζ_0.
(iii) The algorithm is robust. It has a built in noise filtering capability.
(iv) The algorithm incorporates integral action. The errors are reduced to a minimum after the algorithm converges to a solution.

Also, the algorithm is easy to implement on-line and requires a small computation time. Clearly, the MGA performs better than the IMC and PI controllers.

We allow an hour for the performance of the controllers to stabilize and compare the subsequent behaviour of the IMC, PI and MGA controllers. This lets us compare the MGA controller, after its predictive component has converged, to the IMC and PI controllers. Here we find that the standard deviation in the dissolved oxygen concentration from the desired set point of 50% saturation is 3.09 for the IMC controller, 2.797 for the classical PI controller and 1.053 for the MGA controller. Clearly, the converged MGA controller performs better than the PI and IMC controllers.

3.2. *Set point tracking*

As in the previous section the same controllers setting shown in Table 2 are used. The tracking characteristics of the three different controllers are monitored for about 6 h. Here a random multiplicative noise of 2% is incorporated in the dissolved oxygen measurements being transmitted to the controller. Identical conditions are maintained for each of the control strategies and the set

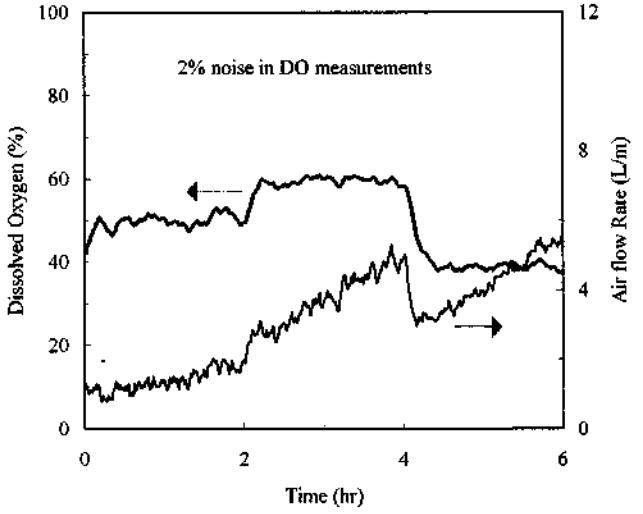

Fig. 6. Set point tracking characteristics of the IMC controller with 2% noise in the dissolved oxygen measurements. Step-up from 50% (0–2 h) to 60% (2–4 h) then step down to 40% (4–6 h).

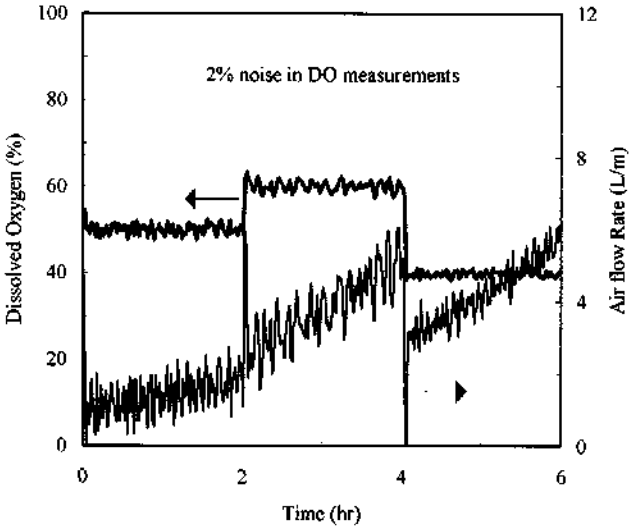

Fig. 7. Set point tracking characteristics of the PI controller with 2% noise in the dissolved oxygen measurements. Step-up from 50% (0–2 hrs) to 60% (2–4 hrs) then step down to 40% (4–6 hrs).

Table 3
Comparison of the set point tracking performances of the IMC, PI and MGA controllers

Controller	σ for 0–2 h (50%)	σ for 2–4 h (60%)	σ for 4–6 h (40%)
IMC	1.285	0.770	0.715
PI	1.169	1.177	0.727
MGA	0.733	0.348	0.262

point tracking experiment conducted in the following manner. The initial dissolved oxygen concentration is 40%. The experiment begins with a step change to 50%. We then control the fermentation at 50% for the first two hours. A step change to 60% is initiated at this point. The process is then at 60% for the next two hours after which the set point is stepped down to 40%. Finally, we control the process at 40% till the end of the set point tracking experiment.

The IMC shows a better performance here compared to its performance in the regulator problem with 5% noise. Although the control action still contains some erratic behaviour, the trend in the air flow rate to meet increasing oxygen demand is clear (Fig. 6). The sharp changes in the air flow rate at the 2 and 4 h mark indicates that the controller recognizes changes in the set point immediately. We observe no overshoot when the IMC moves the process to the new set points for dissolved oxygen. The time required for converging to the new set points is approximately 0.6 hours. The standard deviation of the dissolved oxygen values (before incorporating noise) for each 2 h period, using data after convergence are, 1.286, 0.770 and 0.715, respectively. In Table 3 we present this data for the IMC, PI and MGA controllers.

The classical PI controller shows the fastest response to set point changes among the three controllers. Rapid changes occur in the control action because the PI controller is sensitive to the 2% noise incorporated in the dissolved oxygen readings. Here also, the trend in the air flow rate is evident (Fig. 7). Convergence of the controller occurs in about 0.1 h. However, this advantage is offset by the extremely rapid changes in the control action observed in the air flow rate. For the classical PI controller, the standard deviation of the dissolved oxygen values (before incorporating noise) after 0.1 h for each set point range are 1.169, 1.177 and 0.727, respectively. These values indicate that although the PI controller performs better than the IMC controller during the first set point range, its performance is below that of the IMC controller in the second and third set point range.

In Fig. 8 we present the performance of the MGA controller. Fig. 8 shows clearly that once the MGA has converged, it is capable of controlling the dissolved oxygen very close to the desired set point. The initial oscillations decay in about 0.75 h after start up. The algorithm computes air flow rate values which result in a distinctly smoother profile than the IMC and PI controllers. The variations in the dissolved oxygen concentration from the set point are small after 0.5 h of a step change. The standard deviation values from the set point (before incorporating noise), after convergence of the MGA are, 0.733, 0.348 and 0.262, respectively. These values are significantly lower than both the IMC and PI controllers (Table 3). Thus, the set point tracking capability of the MGA is also superior to that of the IMC and the PI controllers.

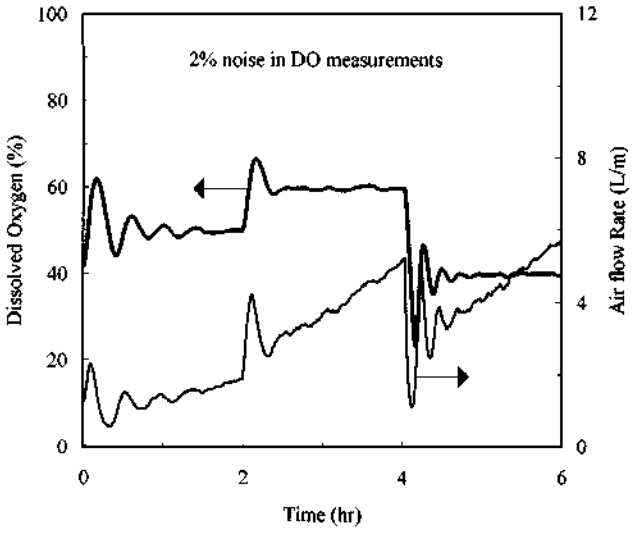

Fig. 8. Set point tracking characteristics of the MGA controller with 2% noise in the dissolved oxygen measurements. Step-up from 50% (0–2 hrs) to 60% (2–4 hrs) then step down to 40% (4–6 hrs).

4. Dissolved oxygen control in *E. coli* and *Streptomyces* fermentations using MGA

The MGA was tested experimentally in *E. coli* and *Streptomyces* fermentations. These experiments demonstrate the capability of the algorithm in real-time implementation (Gomes & Menawat, 1999). Two experiments are presented here. In the first experiment, the MGA controls the dissolved oxygen concentration at 60% in an *E. coli* fermentation and in the second, the MGA controls the dissolved oxygen at 50% in Spectinomycin fermentation by a *Streptomyces* species. In both fermentation experiments we also implemented a modified version of the MGA to control the pH of the fermentations (the derivation of the modified MGA is not presented here).

The software written for data acquisition and control displays the pH, the dissolved oxygen concentration, the temperature and the air flow rate in real time. It has several other features such automatic startup and shut down procedures, function key implementation for specific procedures, and interactive and on-line set-point changing capabilities. Data and associated information are recorded automatically for subsequent data reduction and analysis. The graphic display may be modified according to the requirements of the process. These features are invaluable in monitoring the fermentation process. Fig. 9 presents the basic structure of the control program.

4.1. Performance in E. coli fermentation

We set up the *E. coli* fermentation in the following manner. A slant was plated on a nutrient agar petri dish

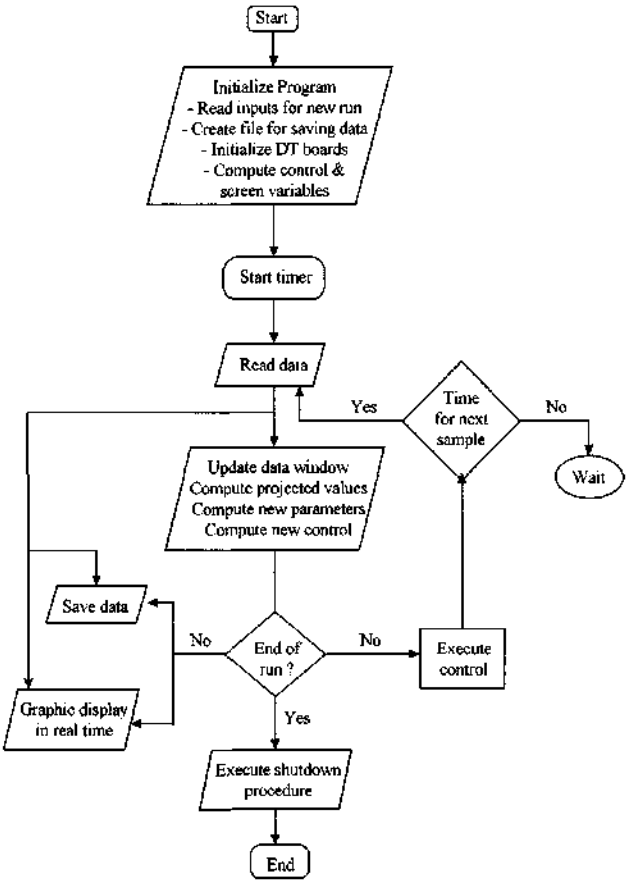

Fig. 9. Structure of the control software.

and incubated for approximately 24. This resulted in thick growth and ensured viability. The seed culture medium was prepared by transferring the *E. coli* from the dish into two 500 ml flasks each containing 250 ml of nutrient broth. After incubating the flasks for 8 h, the seed culture medium was transferred into a 15 l B-Braun fermenter containing 7.5 l of nutrient broth media. Sterile procedures were observed during all transfers and handling of the bacteria. We implemented the MGA to control the dissolved oxygen and pH through a 386 IBM personal computer interfaced to the B-Braun fermenter. The B-Braun temperature control module was used to maintain the fermentation temperature at 37°C and the agitation was set at 200 rpm. The pH, temperature, dissolved oxygen concentration, air flow rate and time duration of acid and base addition were monitored on-line.

The dissolved oxygen, air flow rate and the pH data recorded on-line for controlling the fermentation at a constant 60% and pH at 7 are presented in Fig. 10. During the growth phase, large amounts of oxygen are required for substrate utilization. The gradual increase in the air flow rate to a maximum at about 1.5 h reflects this characteristic. After crossing the maximum, the air flow rate gradually decreases, goes through a minimum and

shows and increasing trend in the latter part of the fermentation. We speculate that once the primary nutrient is consumed the microorganism shifts its metabolic pathway in which the oxygen requirements are higher.

We observe oscillations during the startup phase of the fermentation which takes about 2 h to settle down. The reason for this prolonged oscillation are several. Since the dissolved oxygen concentration is controlled only by manipulating the air flow rate (one sided control), any increase in the dissolved oxygen concentration caused by a change in the air flow rate can drop only when consumed by the microorganism. Other factors include valve hysteresis and insensitivity in the lower range of the air flow rate. However, the magnitude of the oscillations remain within a range of ± 10%. It is important to note that the oscillations become insignificant after about 2.5 hours.

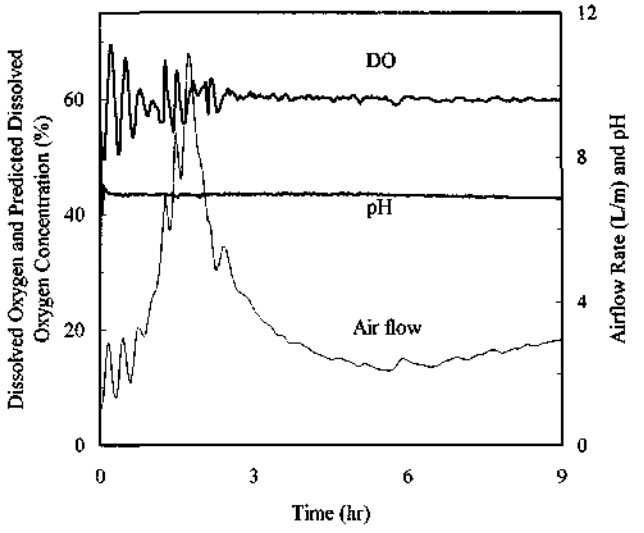

Fig. 10. Dissolved oxygen control in *E. coli* fermentation with the MGA. Set point = 60% dissolved oxygen. pH controlled at 7 with modified MGA.

4.2. Performance in spectinomycin fermentation by streptomyces

Streptomyces being a slow growing species requires a longer period for setting up the experiment. First, a slant incubated for 24 h at 32°C was plated on two petri dishes. The dishes sporulated in about four days when incubated at 32°C. Next, two flasks of 250 ml seed culture medium were prepared. The seed culture medium contained cotton seed flower, brewers yeast, glucose and an antifoaming agent. The seed culture medium was inoculated with healthy spores from the dishes and incubated at 32°C for 33–36 h to obtain a heavy inoculum. Finally, a 15 l B-Braun fermenter containing 5.5 l of production medium was inoculated with 500 ml of seed culture medium prepared for spectinomycin fermentation. The production medium contains the same constituents as the seed culture medium but at a different composition. The only additional component in the production medium was potassium sulphate. The temperature was controlled at 28°C with the B-Braun temperature control module and the agitation was fixed at 400 rpm. The pH was controlled at 6.75 within ± 0.05 using the modified version of the MGA using sulphuric acid and ammonium hydroxide.

Within 24 h the fermentation broth becomes thick and viscous and acquires a muddy appearance. At this point we begin feeding glucose. We observed that as the fermentation progresses and Spectinomycin is produced, the viscosity gradually reduces and the colour of the broth darkens. Fig. 11 shows the performance of the

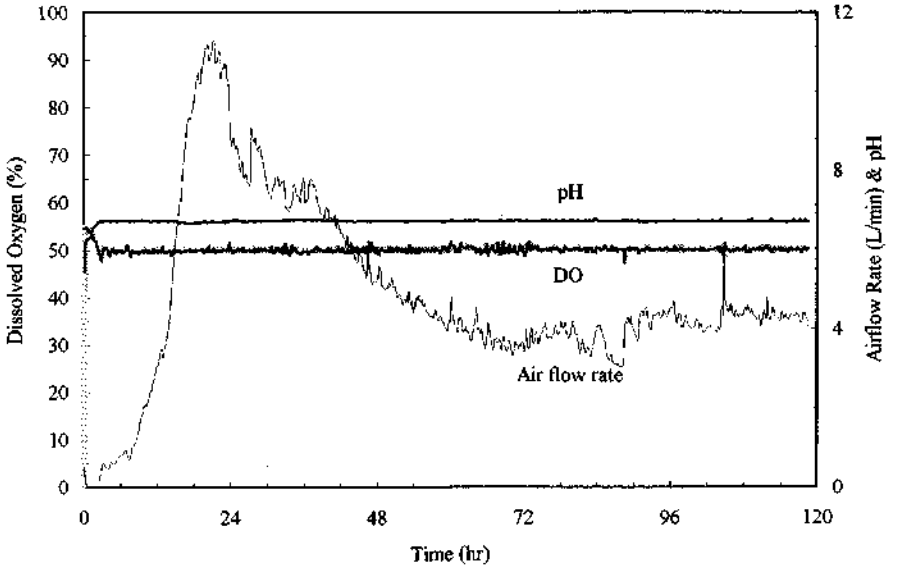

Fig. 11. Dissolved oxygen and pH control of Spectinomycin fermentation. Dissolved oxygen set point = 50% and pH set point = 6.75.

MGA during Spectinomycin fermentation. The MGA exhibits excellent control characteristics in controlling the dissolved oxygen at 50%. Even with a default initial condition of 0% the algorithm converges rapidly to the true values. After the predictive component of the algorithm converges, the deviation of the dissolved oxygen concentration from the set point of 50% are negligible and imperceptible on the graphical display (see Fig. 11). The predicted and true values of dissolved oxygen are within 0.1%. The air flow rate profile clearly indicates the changing requirements for oxygen during the fermentation. Some idea about the changing patterns in cellular metabolism between the tropophase (growth) and the idiophase (production) can be ascertained.

5. Conclusions

In this paper we derived a new Model-Based Geometric Algorithm for controlling fermentations using the geometric representation (Eq. (1)) of fermentation processes. Derivation based on this representation apply to any convenient structure of $f(x)$, $g(x)$ and $h(x)$. The only constraints on the algebraic structure are that $f(x)$ and $g(x)$ must be differentiable and $h(x)$ must be a continuous function. Since the algorithm is derived on a general system representation, in this sense it may be considered as model independent.

The algorithm has been tested in two stages. In the first stage, the simulations were conducted and the performance of the algorithm was compared with the performance of an IMC and a classical PI controller. The results demonstrated that the MGA performs better than the IMC and PI controllers. However, the MGA exhibits an initial period of oscillation because the control implemented is one sided. Also, it requires time for the predictive component of the algorithm converge. In the second stage, the MGA was implemented in *E. coli* and *Streptomyces* fermentations for controlling the dissolved oxygen at a predetermined value. The experimental results clearly show that the MGA is adaptive, robust, incorporates an integral component and converges within a finite number of steps. Its successful implementation in complex mycelial fermentations which are seriously affected by oxygen transfer problems demonstrates the capability of the algorithm.

6. For further reading

The following reference is also of interest to the reader: Slininger et al., 1991.

Acknowledgements

This work was performed in the Department of Chemical Engineering, Tulane University, New Orleans. The research was supported in part by the Abbott Laboratories and by the Sigma Xi Grants in Aid for Research. The author gratefully acknowledges the help of Dr. P. K. Roychoudhury in shaping this paper.

References

Bastin, G., & Gevers, M. R. (1980). Stable adaptive observers for nonlinear time-varying systems. *IEEE Transactions on Automatic Control, 33*, 650–658.

Chattaway, T., & Stephanopoulos, G. (1989). Adaptive estimation of bioreactors: Monitoring plasmid instability. *Chemical Engineering Science, 44*, 41–48.

Chen, H. C., & Wilde, F. (1991). The effect of dissolved oxygen and aeration rate on antibiotic production of *Streptomyces fradiae*. *Biotechnology and Bioengineering, 37*, 591–595.

Cohen, G. H., & Coon, G. A. (1953). Theoretical considerations of retarded control. *Transactions of ASME, 75*, 827.

Contois, D. (1959). Kinetics of bacterial growth relationship between population density and specific growth rate of continuous cultures. *Journal of General Microbiology, 21*, 40–50.

Cooney, C. L., Wang, H. Y., & Wang, D. I. C. (1977). Computer-aided balancing for prediction of fermentation parameters. *Biotechnology and Bioengineering, 19*, 55–67.

Dourado, A., & Calvet, J. L. (1983). Static optimization of ethanol production in a cascade reactor. In A. Halme, *Modelling and control of biotechnical processes*. Oxford.

Ge, S. S., & Lee, T. H. (1997). Robust adaptive neural network control for a class of non-linear systems. *Proceedings of the Institution of Mechanical Engineers, 211*(1), 171–181.

Gomes, J., & Menawat, A. S. (1998). Fed-batch Bioproduction of Spectinomycin. *Advances in Biochemical Engineering and Biotechnology, 59*, 1–46.

Gomes, J., & Menawat, A. S. (1992). Estimation of parameters using partial data. *Biotechnology Progress, 8*, 118–125.

Grootjen, D. R. J., van der Lans, R. G. J. M., & Luyben, K. Ch. A. (1990). Effects of the aeration rate on the fermentation of glucose and xylose by *Pichia stipis* CBS 5773. *Enzyme Microbiological Technology, 12*, 20–23.

Hermann, R., & Krener, A. J. (1977). Nonlinear controllability and observability. *IEEE Transaction Automatic Control, AC-22*(5), 728–740.

Hirschorn, R. M. (1979). Invertibility of multivariable nonlinear control systems. *IEEE Transaction Automatic Control, AC-24*(6), 855–865.

Holmberg, A. (1982). On the practical identifiability of microbial growth models incorporating Michaelis-Menten type nonlinearities. *Mathematical Biosciences, 62*, 23–43.

Holmberg, A., & Ranta, J. (1982). Procedures for parameter and state estimation of microbial growth process models. *Automatica, 13*, 181–193.

Jackson, J. V., & Edwards, V. H. (1975). Kinetics of substrate inhibition if exponential yeast growth. *Biotechnology and Bioengineering, 17*, 943–964.

Johnson, A. (Ed.). (1985). Modelling and control of biotechnological processes. In *Proceedings of the first IFAC symposium*, Noordwijkerhout, The Netherlands: Pergamon Press.

Jurdjevic, V. (1970). Abstract control systems: Controllability and ob servability. *SIAM Journal of Control, 8*(3), 424–439.

Lawford, H., & Rousseau, J. (1989). Effect of oxygen on the rate of β-1, 3-glucan microbial exopolysaccharide production. *Biotechnology Letters, 11*, 125–130.

Lübbert, A., & Simutis, R. (1994). Using measurement data in bioprocess modelling and control. *Trends in Biotechnology, 12*, 304–311.

Massimo, C. Di., Saunders, A. C. G., Morris, A. J., & Montague, G. A. (1989). Non-linear estimation and control of mycelial fermentations. Proceedings of ACC, Pittsburg.

Monod, J. (1942). *Recherches sur la croissance des cultures bactériennes*. Paris: Hermann.

Morari, M., & Zafiriou, E. (1989). *Robust process control*. Englewood Cliffs, NJ: Prentice-Hall.

Moser, H. (1958). *The dynamics of bacterial populations in the chemostat*. Carnegie Inst. Publication, n 614, Washington.

Mou, D. G., & Cooney, C. L. (1983). Growth monitoring and control through computer-aided on-line mass balancing in fed-batch penicillin fermentation. *Biotechnology and Bioengineering, 25*, 225–255.

Munack, A., & Posten, C. (1989). Design of optimal dynamical experiments for parameter estimation. *Proceeding of ACC*, Pittsburg.

Olsson, G. (1976). State of art in sewage treatment plant control. *A.I.Ch.E. Symposiom Series, 72*, 52–76.

Peringer, P., Blachere, H., Corrieu, G., & Lane, A. G. (1972). Mathematical model of the kinetics of growth of *Saccharomyces cerevisiae*. *Fourth international fermentation symposiom*, Kyoto, Japan.

Pomerleau, Y., & Perrier, M. (1990). Estimation of multiple specific growth rates in bioprocesses. *A.I.Ch.E. Journal, 36*, 207–215.

Pomerleau, Y., Perrier, M., & Dochain, D. (1989). Adaptive nonlinear control of the bakers yeast fed-batch fermentation. *Proceedings of ACC*, Pittsburg.

Powell, E. (1967). Growth rate of microorganisms as a function of substrate consumption. Microbial Physiology and Continuous Culture, London: third Symposiom HMSO.

Preez, J. J., du van Driessel, B., & Prior, B. A. (1989). D-xylose fermentation by *Candida shehatae* and *Pichia stipis* at low dissolved oxygen levels in fed-batch cultures. *Biotechnology Letters, 11*, 131–136.

Proll, T., & Karim, N. M. (1994). Nonlinear control of a bioreactor model using exact and I/O linearization. *International Journal of Control, 4*, 499–519.

Riege, P., Blasig, R., Müller, H. G., Heidenreich, G., & Bauch, J. (1989). Influence of oxygen and substrate supply on the metabolism of Candida maltosa during cultivation on n-alkanes. *Applied Microbiology Biotechnology, 32*, 101–107.

Rivera, D. E., Morari, M., & Skogestad, S. (1986). Internal model control, 4. PID controller design. *Industrial Engineering Process Design and Developments, 25*, 252.

Rivlin, T. J. (1981). *An introduction to the approximation of functions*. New York, NY: Dover.

Rollins, M. J., Jensen, S. E., Wolfe, S., & Westlake, D. W. S. (1990). Oxygen depresses deacetooxycephalosporin C synthase and increases the conversion of penicillin N to cephamycin C in *Streptomyces clavuligerus*. *Enzyme Microbiological Technology, 12*, 40–45.

Rollins, M. J., Jensen, S. E., & Westlake, D. W. S. (1989). Regulation of antibiotic production by iron and oxygen during defined medium fermentation of *Streptomyces clavuligerus*. *Applied Microbiology Biotechnology, 31*, 390–396.

Rollins, M. J., Jensen, S. E., & Westlake, D. W. S. (1988). Effect of aeration on antibiotic production by *Streptomyces clavuligerus*. *Journal of Industrial Microbiology, 3*, 357–364.

Scott, R. I., Sladen, S., Maidment, M., Rashid, T., Pratsis, C., & Perry, D. (1980). The effects of oxygen on β-lactam biosynthesis by alginate entrapped *Streptomyces clavuligerus*. *Journal of Chemical Technology and Biotechnology, 41*, 145–154.

Shimizu, H., Takamatsu, T., Shioya, S., & Suga, K. I. (1989). An algorithm approach to constructing the on-line estimation system for the specific growth rate. *Biotechnology and Bioengineering, 33*, 354–364.

Siano, S. A., & Mutharasan, R. (1991). NADH fluorescence and oxygen uptake responses of hybridoma cultures to substrate pulse and step changes. *Biotechnology and Bioengineering, 37*, 141–159.

Slininger, P. J., Branstrator, L. E., Bothast, R. J., Okos, M. R., & Ladisch, M. R. (1991). Growth, death and oxygen uptake kinetics of *Pichia stipitis* on xylose. *Biotechnology and Bioengineering, 37*, 973–980.

Stephanopoulos, G., & San, K. Y. (1984). Studies on on-line bioreactor identification. I. theory. *Biotechnology and Bioengineering, 26*, 1176–1188.

Stoer, J., & Bulirsch, R. (1980). *Introduction to numerical analysis*. New York: Springer.

Swartz, J. R., & Cooney, C. L. (1979). Indirect fermentation measurements as basis for control. *Biotechnology and Bioengineering Symposiom, 9*, 95–101.

Tessier, G. (1942). *Croissance des populations bactériennes et quantités d'aliments disponibles. Review Science Paris* , 80–209.

Wang, H. Y., Cooney, C. L., & Wang, D. I. C. (1979). Computer control of baker's yeast production. *Biotechnology and Bioengineering, 21*, 975–995.

Wang, N. S., & Stephanopoulos, G. A. (1984). New approach to bioprocess identification and modeling. *Biotechnology and Bioengineering Symposiom, 14*, 635–656.

Wecker, A., & Onken, U. (1991). Influence of dissolved oxygen concentration and shear rate on the production of pullulan by Aureobasidium pullulans. *Biotechnology Letters, 13*, 155–160.

Williams, D., Yousefpour, P., & Swanick, B. H. (1984). On-line adaptive control of a fermentation process. *IEE Proceedings, 131*, 117–124.

Yegneswaran, P. K., Gray, M. R., & Thompson, B. G. (1991a). Experimental simulation of dissolved oxygen fluctuations in large fermentors: effect on Streptomyces calvuligerus. *Biotechnology and Bioengineering, 38*, 1203–1209.

Yegneswaran, P. K., Thompson, B. G., & Gray, M. R. (1991b). Effect of dissolved oxygen control on growth and antibiotic production in *Streptomyces clavuligerus*. *Biotechnology Progress, 7*, 246.

Yegneswaran, P. K., Gray, M. R., & Westlake, D. W. S. (1988). Effects of reduced oxygen on growth and antibiotic production in *Streptomyces clavuligerus*. *Biotechnology Letters, 10*, 479–484.

Zhang, Q., Reid, J. F., Litchfield, J. B., Ren, J., & Chang, S. W. (1994). A prototype neural network supervised control system for *Bacillus thuringiensis fermentations*. *Biotechnology and Bioengineering, 43*, 483–489.